# Attosecond photoionization for reconstruction of bound-electron wave packets

Candong Liu,[1] Zhinan Zeng,[1] Ruxin Li,[1,*] Zhizhan Xu,[1] and Mauro Nisoli[2,3,†]

[1]*State Key Laboratory of High Field Laser Physics, Shanghai Institute of Optics and Fine Mechanics, Chinese Academy of Sciences, Shanghai 201800, China*

[2]*Department of Physics, Politecnico di Milano, Piazza Leonardo da Vinci 32, 20133 Milano, Italy*

[3]*Institute of Photonics and Nanotechnologies, IFN-CNR, Piazza Leonardo da Vinci 32, 20133 Milano, Italy*

(Received 28 April 2014; published 3 July 2014)

We present a method for the characterization of bound-electron wave packets generated by a broadband excitation pulse. The technique is based on the photoionization of the electron wave packet by a delayed isolated attosecond pulse and on the measurement of the ionization asymmetry parameter in the direction of the probe pulse polarization, which depends on the pump-probe delay and on the photoelectron energy. By numerically solving the fully three-dimensional time-dependent Schrödinger equation we show that Fourier analysis of the two-dimensional ionization asymmetry parameter, displaying a complex interference pattern, enables a clear observation of quantum beats between pairs of stationary states involved in the generation of the wave packet. An analytical model confirms that the quantum beats' signal encodes the weight of each stationary state, thus suggesting a feasible approach for the complete characterization of the relative population ratio of the excited-state components of the wave packet. Moreover, an approach based on the further analysis of quantum beats is proposed to retrieve the lifetime added to each excited state.

DOI: 10.1103/PhysRevA.90.013403 PACS number(s): 32.80.Rm, 42.65.Ky, 42.65.Re

## I. INTRODUCTION

The excitation of atoms and molecules by broadband extreme ultraviolet (XUV) pulses results in the creation of localized electron wave packets (EWPs), which can be expressed as a coherent superposition of several stationary states. The temporal evolution of the generated EWP is directly related to the energy spacing between the stationary states involved in the coherent superposition. Various techniques have been proposed for complete reconstruction of such wave packets, including (i) attosecond transient absorption spectroscopy [1–3]; (ii) all-optical methods based on the measurement of the modulation of high-harmonic spectrum generated by single-electron recollision [4] and by scanning the pump-probe delay [5]; (iii) use of chirped attosecond pulses [6]; and (iv) measurement of an asymmetry parameter in the attosecond photoionization of the EWP as a function of the delay between the pulse which generates the coherent superposition and an attosecond probe pulse [7–9]. We have recently demonstrated that the measurement of two ionization asymmetry parameters enables one to monitor the temporal evolution of the population of the atomic states involved in the EWP formation [10]. In all these cases, only two stationary states were involved in the coherent superposition.

Shake-up processes [11,12] following the release of core electrons can lead to the generation of EWPs including a series of bound states, whose dynamics is more complex than in the case of two atomic states. EWPs produced by the superposition of a series of bound states have been generated by isolated attosecond pulses [13] or harmonic pulse trains [14] with central photon energy around the ionization threshold. The EWP was then characterized using attosecond electron interferometry [15], which can be also extended to retrieve both time-dependent amplitudes and phases of each stationary state involved in the formation of the EWP, as recently theoretically suggested [16]. This interferometric technique, also referred to as quantum-state holography, requires the use of a broadband attosecond pump pulse for the simultaneous generation of the bound EWP and of a continuum wave packet, which acts as a reference.

In this work we propose a method for the characterization of an EWP generated by the coherent superposition of various atomic stationary states. We assume that the wave packet is generated by a broadband attosecond pulse, below the ionization potential of the atom. The method is based on the use of a second isolated attosecond pulse, which photoionizes the bound EWP, and on the measurement of the ionization asymmetry in the direction of the probe pulse polarization. The numerical solution of the fully three-dimensional (3D) time-dependent Schrödinger equation (TDSE) is performed to obtain the angle-resolved photoelectron spectrum. A method to observe quantum beats between pairs of stationary states by calculating the photoionization asymmetry parameter as a function of the electron energy and the pump-probe delay is presented. We also show that the quantum beat signal encodes the relative population ratio between the excited states. Moreover, we propose an approach to retrieve the lifetime of each excited state.

## II. THEORETICAL MODEL AND NUMERICAL METHODS

We consider the helium atom within the single-active-electron (SAE) approximation model, which has already been used in many previous works [17–19]. The hydrogenic helium atom is prepared by a broadband pump pulse into a coherent superposition of more than two stationary states by single-photon excitation. In particular we will concentrate on the coherent superposition of four states, $1s$, $2p_0$, $3p_0$, and $4p_0$, characterized by the atomic orbitals $\psi_1(\mathbf{r})$, $\psi_2(\mathbf{r})$, $\psi_3(\mathbf{r})$, and $\psi_4(\mathbf{r})$, respectively. Therefore, the generated wave packet

*ruxinli@mail.shcnc.ac.cn
†mauro.nisoli@polimi.it

 

can be written as

$$\psi(\mathbf{r},t) = \alpha_1\psi_1(\mathbf{r}) + \alpha_2 e^{-i\gamma(t)}\psi_2(\mathbf{r}) + \alpha_3 e^{-i\beta_3 - i\gamma(t)\frac{\Delta I_{13}}{\Delta I_{12}}}\psi_3(\mathbf{r}) + \alpha_4 e^{-i\beta_4 - i\gamma(t)\frac{\Delta I_{14}}{\Delta I_{12}}}\psi_4(\mathbf{r}), \quad (1)$$

where $\alpha_i^2$ $(i = 1,2,3,4)$ is the initial population for the $i$th atomic orbital ($\sum_{i=1}^{4}\alpha_i^2 = 1$), $\beta_j$ $(j = 2,3,4)$ is the initial phase depending on the excitation scheme, $\Delta I_{ij} = I_i - I_j$ $(i,j = 1,2,3,4)$ is the energy difference between two atomic states ($i$ and $j$), and $\gamma(t) = \Delta I_{12}t + \beta_2$ is the time-dependent phase shift. Here $I_i$ is the ionization energy of each atomic state. To simplify the notation, the subscripts 1, 2, 3, and 4 in Eq. (1) represent $1s$, $2p_0$, $3p_0$, and $4p_0$, respectively. The exponential terms in Eq. (1) represent the temporal evolution of the wave packet.

The theoretical approach is based on the numerical solution of TDSE as described in Ref. [10]. In the SAE approximation and the Cartesian spherical coordinates, the fully 3D TDSE is given by

$$i\frac{\partial}{\partial t}\psi(\mathbf{r},t) = \left[-\frac{1}{2}\frac{1}{r^2}\frac{\partial}{\partial r}r^2\frac{\partial}{\partial r} + \frac{\hat{l}^2}{2r^2} + V(r) + V_I(\mathbf{r},t)\right] \times \psi(\mathbf{r},t), \quad (2)$$

where $\hat{l}^2$ is the square of the orbit angular momentum operator, $V(r)$ is an effective Coulomb potential with spherical symmetry, and $V_I(\mathbf{r},t)$ is the interaction Hamiltonian for the atom irradiated by the probe XUV pulse. Unless otherwise indicated, atomic units are used throughout: $e = \hbar = m_e = 1$, where $e$ and $m_e$ are the electron charge and mass, respectively. In the length gauge and in the dipole approximation, the interaction Hamiltonian between the hydrogenic helium atom and an isolated attosecond pulse with a linear polarization along the $z$ axis can be described as $V_I(\mathbf{r},t) = zE_z(t)$, where the electric field is written as $E_z(t) = -\frac{dA_z(t)}{dt}$. Here the general expression for the vector potential $A_z(t)$ of a chirped Gaussian attosecond pulse is given by [20]

$$A_z(t) = Re\left(-i\frac{1}{\omega_0}\sqrt{\frac{I_0}{1-i\xi}}\exp\left\{-i[\omega_0(t-t_0)+\varphi_0] - 2\ln 2\frac{(t-t_0)^2}{\tau^2(1-i\xi)}\right\}\right), \quad (3)$$

where $t_0$ is the temporal coordinate corresponding to the peak position of the pulse envelope ($t_0 = 0$ in this work), $\omega_0$ is the central carrier frequency at $t = t_0$, $\xi$ is the dimensionless linear chirp rate, $\varphi_0$ is the carrier envelope phase (CEP), and $I_0$ and $\tau$ are the peak intensity and duration (full width at half maximum) of the transform-limited pulse ($\xi = 0$). While the duration and peak intensity of the pulse, whose vector potential is given by Eq. (3), depend on the chirp rate, $\xi$, the corresponding spectral profile and energy do not depend on $\xi$.

The numerical solution of Eq. (2) is based on the expansion of time-dependent wave function $\psi(\mathbf{r},t)$ in series of partial waves indexed by angular quantum number $l$ and magnetic quantum number $m$, i.e.,

$$\psi(\mathbf{r},t) = \sum_{l=0}^{+\infty}\sum_{m=-l}^{l}\frac{1}{r}\varphi_{lm}(r,t)Y_l^m(\theta,\phi). \quad (4)$$

In this way Eq. (2) can be written as a set of coupled equations between the different angular quantum numbers for the radial wave function $\varphi_{lm}(r,t)$ [10]. Here we employ the finite-element discrete variable representation method to discretize the radial equations due to the advantage of forming the block-diagonal sparse matrix representation of the kinetic operator and the diagonal matrix representation of the effective Coulomb potential [21,22]. The temporal evolution of the wave function is carried out by the Arnoldi-Lanczos algorithm [23].

The projection of the final wave function onto the field-free scattering state $\psi_{\mathbf{p}}^{C}(\mathbf{r})$ yields the probability amplitude $a(\mathbf{p})$ of the continuum EWP with momentum $\mathbf{p} = (p,\theta_p,\phi_p)$ generated by the probe XUV pulse, i.e.,

$$a(\mathbf{p}) = \left\langle \psi_{\mathbf{p}}^{C}(\mathbf{r}) \,\middle|\, \psi(\mathbf{r},t_f)\right\rangle. \quad (5)$$

In order to conveniently calculate $a(\mathbf{p})$ and the subsequent differential ionization probability, the helium atom has been approximately treated as a hydrogenlike atom with an attractive Coulomb potential $V(r) = -Z/r$, since in this case the analytical expression for the continuum scattering state $\psi_{\mathbf{p}}^{C}(\mathbf{r})$ is accessible. The net nuclear charge $Z$ is chosen as $Z = 1.3443$ to faithfully reproduce the ground-state energy of the helium atom. Although the excited-state energy slightly deviates from the real value, this does not affect the conclusions of this work. The expression of $\psi_{\mathbf{p}}^{C}(\mathbf{r})$ and an analytical formula for $a(\mathbf{p})$ are given in Ref. [10]. We point out that $a(\mathbf{p})$ does not depend on the azimuth angle, $\phi_p$, due to the axial symmetry of the coherently coupled wave function with respect to the $z$ axis. It follows that the angle-resolved photoelectron energy spectrum can be described by the double differential ionization probability (DDIP):

$$D(\mathcal{E},\theta_p) = \frac{\partial^2 P}{\partial\mathcal{E}\sin\theta_p\partial\theta_p} = 2\pi\sqrt{2\mathcal{E}}|a(\sqrt{2\mathcal{E}},\theta_p,0)|^2, \quad (6)$$

where $\mathcal{E} = p^2/2$ is the kinetic energy of photoelectrons. The absolute energy-dependent differential asymmetry parameter, $A_d(\mathcal{E})$, in the direction of the XUV pulse polarization can be defined as $A_d(\mathcal{E}) = D(\mathcal{E},0) - D(\mathcal{E},\pi)$.

The simulation parameters used in our calculation are the following: The maximum radial distance is $r_{\max} = 150$ a.u. with 300 finite elements and eight basis functions in each element, the maximum angular quantum number is $l_{\max} = 8$, the time step of wave function propagation is $\delta t = 0.01$ a.u., and the Arnoldi-Lanczos propagation order is $M = 40$.

## III. RESULTS AND DISCUSSION

### A. Quantum beats from TDSE calculation

We assume that the prepared EWP, $\psi(\mathbf{r},t)$, is probed by measuring the photoionization induced by an isolated attosecond XUV pulse with variable delay. Note that different phase shifts, $\gamma(t)$, correspond to different pump-probe temporal delays. Equal populations ($\alpha_i^2 = 1/4$) for each stationary state in $\psi(\mathbf{r},t)$ are assumed. The parameters of the attosecond

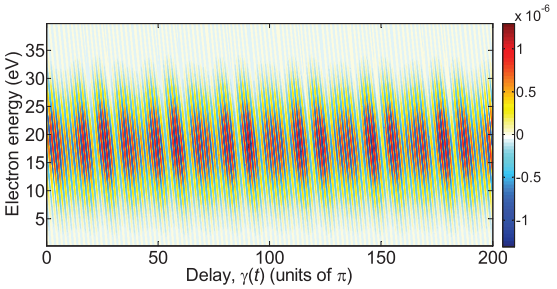


FIG. 1. (Color online) Differential ionization asymmetry parameter, $A_d$, as a function of the electron energy and of the pump-probe temporal delay. Equal populations for $1s, 2p_0, 3p_0$, and $4p_0$ stationary states are assumed in the prepared EWP. The parameters of the probe XUV pulse are peak intensity $I_0 = 1.0 \times 10^{12}$ W/cm$^2$, transform-limited duration $\tau = 130$ as, central photon frequency $\omega_0 = 36$ eV, chirp rate $\xi = 3$, and carrier envelope phase $\varphi_0 = 0$.

probe pulse considered in the calculations are the following: transform-limited peak intensity $I_0 = 1.0 \times 10^{12}$ W/cm$^2$, transform-limited duration $\tau = 130$ as, central photon energy $\omega_0 = 36$ eV, chirp rate $\xi = 3$ (related to the intrinsic chirp of the XUV pulses [24,25]), and CEP value $\varphi_0 = 0$. These pulse parameters can be obtained experimentally by employing, for example, the polarization gating technique [26].

We have first calculated the energy-dependent differential asymmetry parameter, $A_d(\mathcal{E})$, as a function of the temporal delay, $\gamma(t)$: The result is presented in Fig. 1. A series of tilted interference fringes are produced, with different oscillation frequency and time-dependent envelope. The important information embedded in Fig. 1 can be extracted by Fourier analysis of the interferogram. The frequency-energy map shown in Fig. 2(a) has been obtained by calculating the Fourier transform of the asymmetry parameter $A_d$ shown in Fig. 1 along the delay axis at each electron energy. The Fourier map clearly shows quantum beats between three pairs of atomic states. To highlight the quantum beat signal, we performed the integration of Fig. 2(a) along the electron energy axis so that a one-dimensional function of the oscillation frequency is obtained. The calculated result is shown in Fig. 2(b), where the three main peaks are clearly visible, which correspond to the

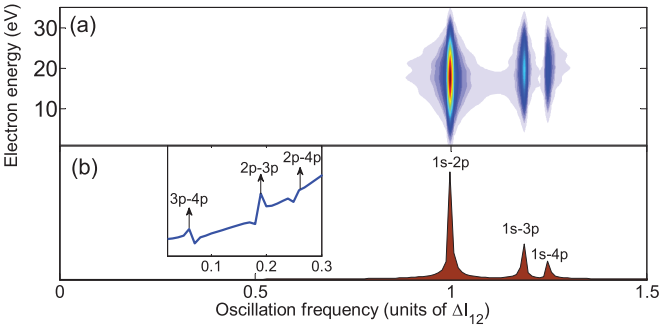


FIG. 2. (Color online) (a) Two-dimensional quantum beats obtained from Fourier transform of the map shown in Fig. 1 along the delay axis at each electron energy. (b) One-dimensional quantum beats obtained by integrating panel (a) along the electron energy axis at each oscillation frequency. Inset is the close-up of quantum beats signal in the region of low oscillation frequencies.

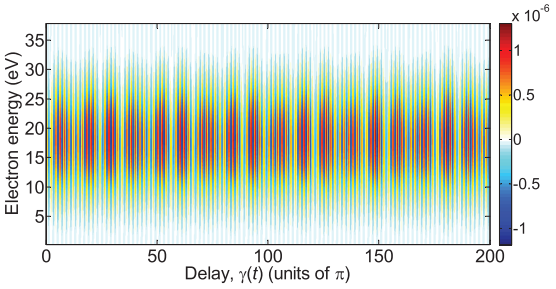


FIG. 3. (Color online) Differential ionization asymmetry, $A_d$, as a function of the electron energy and the pump-probe temporal delay, calculated for chirp rate $\xi = 0$. Other parameters are the same as in Fig. 1.

quantum beat between $1s$-$2p$, $1s$-$3p$, and $1s$-$4p$ pairs of states with opposite parity. In order to measure the quantum beat corresponding to a pair of states with the same parity, spectral overlap between the continuum electron produced from one state by one-photon ionization and from the other state by two-photon ionization is required. In the case of the parameters used in our calculation and due to the small probability of two-photon ionization, the resulting quantum beat signal between identical parity states is rather weak. Indeed, as we expect, the quantum beat between $3p$-$4p$, $2p$-$3p$, and $2p$-$4p$ pairs of states can be observed by magnifying the curve reported in Fig. 2(b) in the region of low frequencies, as shown in the inset of Fig. 2(b). We have also calculated the energy-resolved and delay-dependent asymmetry parameter, $A_d$, for different chirp rates, $\xi$, while keeping other pulse parameters identical. We note that the chirp rate of attosecond pulses can be varied, for example, by using thin metallic filters [27]. It is found that the energy-delay map of $A_d$ exhibits a pattern similar to that shown in Fig. 1, except for the fringe slope, which depends on the chirp rate. In particular, in the case of transform-limited XUV pulses ($\xi = 0$), the fringes become vertical, as reported in Fig. 3. By using the Fourier analysis it is possible to show that the retrieved quantum beat frequencies do not depend on the chirp rate of the attosecond pulse used to probe the EWP.

### B. Analytical investigation

We have then used a simple analytical model to analyze the ionization of the bound EWP by the attosecond probe pulse. For the helium atom, the two-photon double ionization is energetically forbidden for the XUV photon energy lower than 39.5 eV [28]. In our work, the central photon energy of the probe XUV pulse is chosen as 36 eV, leading to the dominant one-photon single ionization. Consequently, we can neglect the influence of the recollision of the computed EWP with the second electron. Assuming that the XUV probe pulse promotes each stationary state of the EWP to the final continuum state, the probability amplitude for the free EWP in the spectral domain can be expressed as

$$M_f(\mathcal{E},\theta_p,t_d) = \sum_{j=1}^{4} \alpha_j M_j(\mathcal{E},\theta_p) \exp[i\phi_j(\mathcal{E},\theta_p) - i\theta_j(t_d)], \quad (7)$$

where $M_j(\mathcal{E},\theta_p)$ and $\phi_j(\mathcal{E},\theta_p)$ are the energy- and angle-dependent amplitude and phase created from the stationary state $j$, respectively. Here $\theta_j(t_d)$ represents the delay-dependent phase, given by $\theta_1(t_d)=0$, $\theta_2(t_d)=\gamma(t_d)$, $\theta_3(t_d)=\frac{\Delta I_{13}}{\Delta I_{12}}\gamma(t_d)+\beta_3$, and $\theta_4(t_d)=\frac{\Delta I_{14}}{\Delta I_{12}}\gamma(t_d)+\beta_4$, where $t_d$ is the temporal delay. Thus the photoelectron spectrum, which is a function of the delay, $t_d$, and of the angle, $\theta_p$, can be written as

$$D(\mathcal{E},\theta_p,t_d)=|M_f(\mathcal{E},\theta_p,t_d)|^2, \tag{8}$$

and the corresponding differential asymmetry parameter is given by

$$A_d(\mathcal{E},t_d)=D(\mathcal{E},0,t_d)-D(\mathcal{E},\pi,t_d). \tag{9}$$

The positive frequency component of the XUV pulse spectrum, obtained by calculating the Fourier transform of $E_z(t)$, is given by $E_+(\omega)=\frac{1}{2}a(\omega)e^{i\eta(\omega)}$ with

$$a(\omega)=\frac{\sqrt{I_0}}{\omega_0}\sqrt{\frac{\pi}{2\ln 2}}\omega\tau\exp\left[-\frac{1}{8\ln 2}(\omega-\omega_0)^2\tau^2\right], \tag{10}$$

and

$$\eta(\omega)=\omega t_0+\frac{\xi\tau^2(\omega-\omega_0)^2}{8\ln 2}-\varphi_0, \tag{11}$$

where $\omega$ gives the XUV photon energy. We consider the dominant single-photon ionization in the case of XUV photon energy above the ionization potential of the target atom. Therefore, the spectrum of the XUV pulse is directly mapped onto the free EWP [29], leading to

$$\phi_j(\mathcal{E},\theta_p)=\eta(\mathcal{E}+I_j), \tag{12}$$

and

$$M_j(\mathcal{E},\theta_p)=S_j(\mathcal{E},\theta_p)a(\mathcal{E}+I_j), \tag{13}$$

where $S_j(\mathcal{E},\theta_p)$ is the ionization amplitude in the monochromatic case. By incorporating Eqs. (7)–(13), we have

$$A_d(\mathcal{E},t_d)=\sum_{j=2}^{4}\alpha_1\alpha_j a(\mathcal{E}+I_1)a(\mathcal{E}+I_j)|S_1(\mathcal{E},0)S_j(\mathcal{E},0)| \times\cos\Delta\Phi_{1j}(\mathcal{E},t_d), \tag{14}$$

where the phase difference between state 1 and state $j$ is given by

$$\Delta\Phi_{1j}(\mathcal{E},t_d)=\Delta I_{1j}\left[t_d+\frac{\xi\tau^2}{4\ln 2}\mathcal{E}\right]+C_{1j}. \tag{15}$$

Here for simplicity the expression of $C_{1j}$ independent of $\mathcal{E}$ and $t_d$ is not written explicitly.

We can see from Eqs. (14) and (15) that the two-dimensional asymmetry parameter, $A_d$, is characterized by an oscillatory pattern as a function of $t_d$, with different frequencies $\Delta I_{1j}$. The position of maxima and minima is given by $\Delta\Phi_{1j}(\mathcal{E},t_d)=n\pi$ ($n=0,\pm1,\pm2,\ldots$), which yields the relationship between $t_d$ and $\mathcal{E}$, i.e., $t_d=k\mathcal{E}+\frac{n\pi-C_{1j}}{\Delta I_{1j}}$ with $k=-\frac{\xi\tau^2}{4\ln 2}$. It is evident that the fringe slope $k$ is proportional to $\xi$. We can analytically calculate for $\xi=3$ the slope value equal to $k=31$, which is in very good agreement with the slope value, $k_e=30$, extracted directly from Fig. 1. Moreover, in the case of transform-limited XUV pulses ($\xi=0$), $t_d=\frac{n\pi-C_{1j}}{\Delta I_{1j}}$, in agreement with the result of Fig. 3 showing vertical fringes. Our results demonstrate the possibility to directly read the linear chirp rate of the isolated attosecond pulse by measuring the fringe slope in the $A_d$ interferogram. The case of states with the same parity cannot be included in this simple analytical model, where only single-photon ionization is considered.

We note that the quantum beats encode information on the population of the states involved in the EWP formation. Indeed, the strength of the one-dimensional quantum beats defined by the integration over $\mathcal{E}$, directly extracted from Eq. (14), can be written as

$$Q_{1j}\propto\alpha_1\alpha_j R_{1j}, \tag{16}$$

with $R_{1j}=\int a(\mathcal{E}+I_1)a(\mathcal{E}+I_j)|S_1(\mathcal{E},0)S_j(\mathcal{E},0)|d\mathcal{E}$ and $j=2,3,4$. It is found that the information about the population of the states involved in the formation of the EWP is encoded in the quantum beat pattern in the form of $\alpha_1\alpha_j$. We concentrate on the relative strength of quantum beats:

$$\frac{Q_{12}}{Q_{13}}=\frac{\alpha_2 R_{12}}{\alpha_3 R_{13}}\quad\text{and}\quad\frac{Q_{12}}{Q_{14}}=\frac{\alpha_2 R_{12}}{\alpha_4 R_{14}}. \tag{17}$$

These expressions suggest a feasible way for the measurement of the relative population ratios $\alpha_2/\alpha_3$ and $\alpha_2/\alpha_4$ between the excited-state components, since $Q_{12}/Q_{13}$ and $Q_{12}/Q_{14}$ can be obtained from the experiment, while $R_{12}/R_{13}$ and $R_{12}/R_{14}$ can be obtained from the calculations. In the example considered in this work the relative height of the peak in Fig. 2(b) gives $Q_{12}/Q_{13}=2.9988$ and $Q_{12}/Q_{14}=5.7558$, while direct calculation gives $R_{12}/R_{13}=2.8570$ and $R_{12}/R_{14}=5.2191$ which are not related with any dynamical process. Consequently, we can obtain the retrieved population ratios $(\alpha_2/\alpha_3)_M=1.0496$ and $(\alpha_2/\alpha_4)_M=1.1028$, in excellent agreement with the real value $\alpha_2/\alpha_3=\alpha_2/\alpha_4=1$.

### C. Lifetime retrieval

It is also possible to demonstrate that the temporal evolution of the EWP can be obtained from the quantum beat map. We have artificially imposed a lifetime for each excited state. For the free propagation of the EWP, the lifetime is introduced by multiplying a decay factor to the excited-state wave function. In this case the temporal evolution of the prepared EWP can be expressed by simply modifying Eq. (1) as follows:

$$\begin{aligned}\psi(\mathbf{r},t)=&\alpha_1\psi_1(\mathbf{r})+\alpha_2 e^{-\frac{\Delta I_{12}t}{2\tau_2}-i\gamma(t)}\psi_2(\mathbf{r})\\&+\alpha_3 e^{-\frac{\Delta I_{12}t}{2\tau_3}-i\beta_3-i\gamma(t)\frac{\Delta I_{13}}{\Delta I_{12}}}\psi_3(\mathbf{r})\\&+\alpha_4 e^{-\frac{\Delta I_{12}t}{2\tau_4}-i\beta_4-i\gamma(t)\frac{\Delta I_{14}}{\Delta I_{12}}}(\mathbf{r}),\end{aligned} \tag{18}$$

where $\tau_2$, $\tau_3$, and $\tau_4$ represent the lifetimes of $2p_0$, $3p_0$, and $4p_0$ states, respectively, in units of $1/\Delta I_{12}$. Equation (18) shows that the probability of finding the electron in a particular excited state decreases with time $t$ as $\exp(-\frac{\Delta I_{12}}{\tau_j}t)$ ($j=2,3,4$). When the EWP interacts with the XUV probe pulse, we take into account the state lifetimes by applying the projection operator,

$$P=1-\sum_{j=2}^{4}\frac{\Delta I_{12}}{2\tau_j}\Delta t|\psi_j(\mathbf{r})\rangle\langle\psi_j(\mathbf{r})|, \tag{19}$$

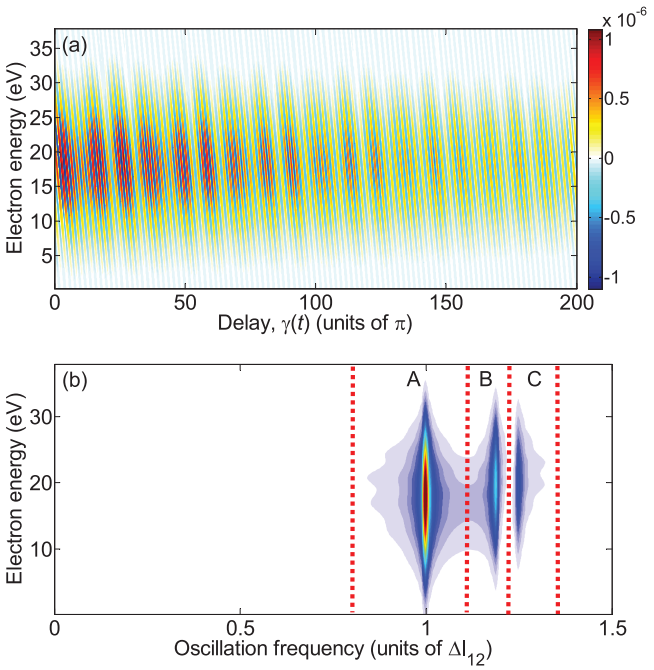


FIG. 4. (Color online) (a) Differential ionization asymmetry, $A_d$, as a function of the electron energy and the pump-probe temporal delay, calculated in the case of the limited lifetime artificially imposed on each excited state. Other simulation parameters are the same as in Fig. 1. (b) Quantum beats obtained from Fourier transform of $A_d$ along the delay axis. The red dashed lines indicate the edges of the filter function that is used to separate the different quantum beat signal. Regions A, B, and C correspond to the beat signals $1s$-$2p$, $1s$-$3p$, and $1s$-$4p$, respectively.

to act on the wave function at each propagation step of the small time interval $\Delta t$, so that the contribution of excited states can be gradually removed from the total wave function. Note that the projection operator originates from the approximation relationship:

$$\exp\left(-\frac{\Delta I_{12}}{2\tau_j}\Delta t\right) \approx 1 - \frac{\Delta I_{12}}{2\tau_j}\Delta t.$$

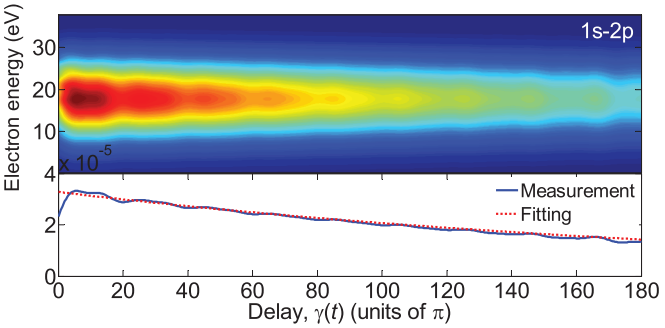


FIG. 5. (Color online) Top: Temporal evolution of the amplitude in the time domain, obtained by performing the inverse Fourier transform of the separated quantum beat $1s$-$2p$. Bottom: Comparison of the measurement signal (blue solid line), which is obtained by integrating the top panel along the electron energy axis, with the fitting curve (red dashed line), which has the function form of $x_1 \exp[-\frac{\gamma(t)}{2x_2}]$.

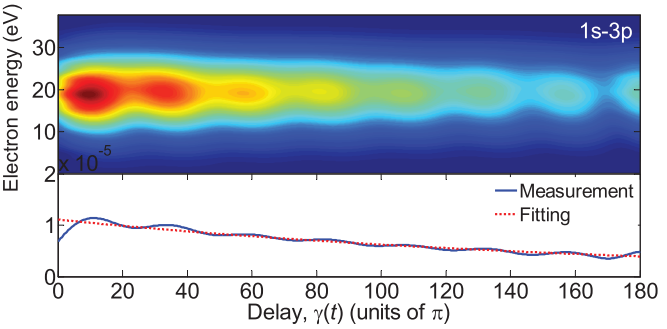


FIG. 6. (Color online) Top: Temporal evolution of the amplitude in the time domain, obtained by performing the inverse Fourier transform of the separated quantum beat $1s$-$3p$. Bottom: Comparison of the measurement signal (blue solid line), which is obtained by integrating the top panel along the electron energy axis, with the fitting curve (red dashed line), which has the function form of $x_1 \exp[-\frac{\gamma(t)}{2x_2}]$.

Let us assume that the lifetime parameters are given by $\tau_2 = 100\pi$, $\tau_3 = 80\pi$, and $\tau_4 = 60\pi$. The asymmetry parameter, $A_d$, can be obtained by exact solution of the 3D TDSE as a function of the electron energy $\mathcal{E}$ and of the pump-probe delay, $\gamma(t)$. The results are reported in Fig. 4(a), which displays a periodic oscillation structure characterized by an amplitude which decreases upon increasing the temporal delay. The Fourier transform of $A_d$ along the delay axis yields the two-dimensional map of quantum beats as a function of the electron energy and the oscillation (Fourier) frequency, as shown in Fig. 4(b). We apply square filter functions, whose edges are denoted as red dashed lines in Fig. 4(b), to separate the quantum beat signal into three different regions A–C corresponding to beats $1s$-$2p$, $1s$-$3p$, and $1s$-$4p$, respectively. Then the quantum beat filtered from one of the regions is inverse Fourier transformed back to the time domain. Since we only filter out the positive frequency component, the inverse Fourier transform should give the temporal evolution of the amplitude information for the separated quantum beat $1s$-$2p$, $1s$-$3p$, and $1s$-$4p$, as shown in the top panel of Figs. 5–7, respectively, which show a clear decay. The corresponding integral signal obtained by summing over the electron energy

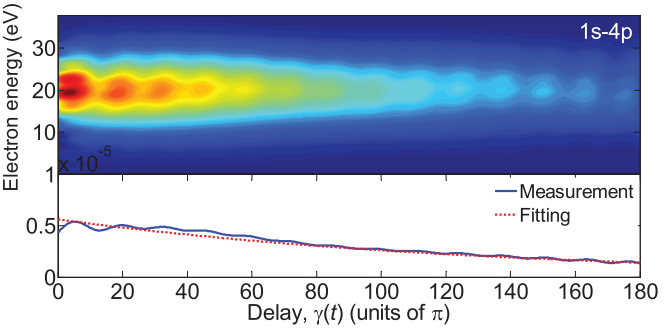


FIG. 7. (Color online) Top: Temporal evolution of the amplitude in the time domain, obtained by performing the inverse Fourier transform of the separated quantum beat $1s$-$4p$. Bottom: Comparison of the measurement signal (blue solid line), which is obtained by integrating the top panel along the electron energy axis, with the fitting curve (red dashed line), which has the function form of $x_1 \exp[-\frac{\gamma(t)}{2x_2}]$.

is plotted by blue solid curves in the bottom panel of Figs. 5–7. We perform the curve fitting of the integral signal with the function form $x_1 \exp[-\frac{\gamma(t)}{2x_2}]$ in order to obtain the lifetime, given by the fitting parameter $x_2$. The fitting results are shown by red dashed curves in the bottom panel of Figs. 5–7, and the retrieved lifetimes are given by $\tau_2 = 108\pi$, $\tau_3 = 86\pi$, and $\tau_4 = 64\pi$, in excellent agreement with the imposed ones. It is worth mentioning that this retrieval approach is universal and only dependent on the observable quantum beats signal, without requiring any prior information on the XUV pulse and on the atomic structure.

## IV. CONCLUSIONS

We have discussed an approach for the characterization of an EWP generated by the coherent superposition of many atomic states. The EWP is probed by an isolated attosecond pulse, which ionizes the wave packet at various temporal delays. By numerically solving the 3D TDSE we have demonstrated that the differential asymmetry parameter in the direction of the polarization of the attosecond probe pulse can be used for the characterization of the EWP. The Fourier analysis of the asymmetry parameter in the energy-delay representation directly shows the quantum beats between pairs of stationary states, thus giving the energy difference between pairs of atomic states and the time scale of the corresponding electronic motion. By using an analytical model, we obtained a quantitative relationship between the fringe slope in the energy-delay map of the asymmetry parameter and the chirp rate of the probe pulse. Moreover, the relative population ratio between excited states and their lifetimes related to the temporal evolution are encoded in the quantum beat signal, so that they can be easily retrieved.

## ACKNOWLEDGMENTS

This work was supported by the National Natural Science Foundation of China (Grants No. 11127901 and No. 61221064), 973 Project (Grant No. 2011CB808103), Shanghai Yangfan Project (Grant No. 14YF1406000), and the European Research Council under the European Community's Seventh Framework Programme (FP7/2007-2013)/ERC Grant Agreement No. 227355 ELYCHE.

[1] E. Goulielmakis, Z. Loh, A. Wirth, R. Santra, N. Rohringer, V. S. Yakovlev, S. Zherebtsov, T. Pfeifer, A. M. Azzeer, M. F. Kling, S. R. Leone, and F. Krausz, Nature (London) **466**, 739 (2010).

[2] A. Wirth, M. Th. Hassan, I. Grguraš, J. Gagnon, A. Moulet, T. T. Luu, S. Pabst, R. Santra, Z. A. Alahmed, A. M. Azzeer, V. S. Yakovlev, V. Pervak, F. Krausz, and E. Goulielmakis, Science **334**, 195 (2011).

[3] R. Santra, V. S. Yakovlev, T. Pfeifer, and Z.-H. Loh, Phys. Rev. A **83**, 033405 (2011).

[4] H. Niikura, D. M. Villeneuve, and P. B. Corkum, Phys. Rev. Lett. **94**, 083003 (2005).

[5] T. Bredtmann, S. Chelkowski, and A. D. Bandrauk, Phys. Rev. A **84**, 021401(R) (2011).

[6] G. L. Yudin, A. D. Bandrauk, and P. B. Corkum, Phys. Rev. Lett. **96**, 063002 (2006).

[7] G. L. Yudin, S. Chelkowski, J. Itatani, A. D. Bandrauk, and P. B. Corkum, Phys. Rev. A **72**, 051401(R) (2005).

[8] S. Chelkowski, G. L. Yudin, and A. D. Bandrauk, J. Phys. B **39**, S409 (2006).

[9] A. D. Bandrauk, S. Chelkowski, P. B. Corkum, J. Manz, and G. L. Yudin, J. Phys. B **42**, 134001 (2009).

[10] C. Liu and M. Nisoli, Phys. Rev. A **85**, 053423 (2012).

[11] M. Uiberacker, Th. Uphues, M. Schultze, A. J. Verhoef, V. Yakovlev, M. F. Kling, J. Rauschenberger, N. M. Kabachnik, H. Schröder, M. Lezius, K. L. Kompa, H.-G. Muller, M. J. J. Vrakking, S. Hendel, U. Kleineberg, U. Heinzmann, M. Drescher, and F. Krausz, Nature (London) **446**, 627 (2007).

[12] V. Schmidt, Rep. Prog. Phys. **55**, 1483 (1992).

[13] J. Mauritsson, T. Remetter, M. Swoboda, K. Klunder, A. L'Huillier, K. J. Schafer, O. Ghafur, F. Kelkensberg, W. Siu, P. Johnsson, M. J. J. Vrakking, I. Znakovskaya, T. Uphues, S. Zherebtsov, M. F. Kling, F. Lepine, E. Benedetti, F. Ferrari, G. Sansone, and M. Nisoli, Phys. Rev. Lett. **105**, 053001 (2010).

[14] K. T. Kim, D. H. Ko, J. Park, N. N. Choi, C. M. Kim, K. L. Ishikawa, J. Lee, and C. H. Nam, Phys. Rev. Lett. **108**, 093001 (2012).

[15] N. N. Choi, T. F. Jiang, T. Morishita, M.-H. Lee, and C. D. Lin, Phys. Rev. A **82**, 013409 (2010).

[16] K. Klunder, P. Johnsson, M. Swoboda, A. L'Huillier, G. Sansone, M. Nisoli, M. J. J. Vrakking, K. J. Schafer, and J. Mauritsson, Phys. Rev. A **88**, 033404 (2013).

[17] M. Geissler, G. Tempea, and T. Brabec, Phys. Rev. A **62**, 033817 (2000).

[18] C. Liu, R. Li, Z. Zeng, Y. Zheng, P. Liu, and Z. Xu, Opt. Lett. **35**, 2618 (2010).

[19] S. Chelkowski, A. D. Bandrauk, and A. Apolonski, Phys. Rev. A **70**, 013815 (2004).

[20] C. Liu and M. Nisoli, Phys. Rev. A **86**, 053404 (2012).

[21] T. N. Rescigno and C. W. McCurdy, Phys. Rev. A **62**, 032706 (2000).

[22] C. Y. Lin and Y. K. Ho, Phys. Rev. A **84**, 023407 (2011).

[23] A. Castro, M. A. L. Marques, and A. Rubio, J. Chem. Phys. **121**, 3425 (2004).

[24] Y. Mairesse, A. de Bohan, L. J. Frasinski, H. Merdji, L. C. Dinu, P. Monchicourt, P. Breger, M. Kovačev, R. Taïeb, B. Carré, H. G. Muller, P. Agostini, and P. Salières, Science **302**, 1540 (2003).

[25] C. Liu, Z. Zeng, Y. Zheng, P. Liu, R. Li, and Z. Xu, Phys. Rev. A **85**, 043420 (2012).

[26] G. Sansone, E. Benedetti, F. Calegari, C. Vozzi, L. Avaldi, R. Flammini, L. Poletto, P. Villoresi, C. Altucci, R. Velotta, S. Stagira, S. De Silvestri, and M. Nisoli, Science **314**, 443 (2006).

[27] R. López-Martens, K. Varjú, P. Johnsson, J. Mauritsson, Y. Mairesse, P. Salières, M. B. Gaarde, K. J. Schafer, A. Persson, S. Svanberg, C.-G. Wahlström, and A. L'Huillier, Phys. Rev. Lett. **94**, 033001 (2005).

[28] H. Bachau, Phys. Rev. A **83**, 033403 (2011).

[29] G. L. Yudin, S. Chelkowski, and A. D. Bandrauk, J. Phys. B **39**, L17 (2006).